Scanning tunneling microscopy of graphene on Ru(0001)

S. Marchini, S. Günther, and J. Wintterlin*
Ludwig-Maximilians-Universität München, Department Chemie, Butenandtstrasse 5-13, 81377 Munich, Germany
(Received 29 November 2006; revised manuscript received 31 July 2007; published 28 August 2007)

After prolonged annealing of a Ru(0001) sample in ultrahigh vacuum a superstructure with a periodicity of ~30 Å was observed by scanning tunneling microscopy (STM). Using x-ray photoelectron spectroscopy it was found that the surface is covered by graphitic carbon. Auger electron spectroscopy shows that between 1000 and 1400 K carbon segregates to the surface. STM images recorded after annealing to increasing temperatures display islands of the superstructure, until, after annealing to $T \geqslant 1400$ K, it covers the entire surface. The morphology of the superstructure shows that it consists of a single graphene layer. Atomically resolved STM images and low-energy electron diffraction reveal an (11×11) structure or incommensurate structure close to this periodicity superimposed by 12×12 graphene cells. The lattice mismatch causes a moiré pattern. Unlike the common orientational disorder of adsorbed graphene, the graphene layer on Ru(0001) shows a single phase and very good rotational alignment. Misorientations near defects in the overlayer only amount to ~1°, and the periodicity of ~30 Å is unaffected. In contrast to bulk graphite both carbon atoms in the graphene unit cell were resolved by STM, with varying contrast depending on the position above the Ru atoms. The filled and empty state images of the moiré structure differ massively, and electronic states at −0.4 and +0.2 V were detected by scanning tunneling spectroscopy. The data indicate a significantly stronger chemical interaction between graphene and the metal surface than between neighboring layers in bulk graphite. The uniformity of the structure and its stability at high temperatures and in air suggest an application as template for nanostructures.

DOI: 10.1103/PhysRevB.76.075429 PACS number(s): 68.35.Dv, 68.37.Ef, 61.46.−w, 73.20.−r

I. INTRODUCTION

In the current research in nanoscience one important goal is to develop templates on which uniform nanostructures can be grown. An ideal template would provide large areas of identical nanoscopic cells and would be easy to prepare, tolerate high temperatures, and be stable under ambient conditions. Recently N'Diaye and collaborators demonstrated that single layer graphite films adsorbed on an iridium surface can serve as templates for metallic nanoparticles.[1] By decomposing ethylene on Ir(111) at 1450 K a (9×9) superstructure was prepared, resulting from the lattice mismatch between graphene, i.e., a single graphite layer, and the Ir surface. Evaporation of Ir onto this surface led to small clusters of Ir atoms in the unit cells of the (9×9) superstructure. Because of the regular graphene superstructure ordered 2D arrays of clusters were obtained in this way. The clusters displayed narrow and tunable size distributions, and they were stable at temperatures up to 500 K.

We have studied graphene layers on the Ru(0001) surface. This system promises to be an ideal candidate as template for nanoparticles. The graphene layer is very simple to prepare, and one can form complete layers with the same structure across the entire crystal. The overlayers are stable at $T \geqslant 1400$ K in vacuum and are unaffected by exposure to air.

An established procedure to prepare graphene layers on surfaces is by decomposition of CO or hydrocarbon molecules on metal surfaces at elevated temperatures.[2–5] This is the same process occurring as an undesired by-reaction in heterogeneous catalysis, where deposits of graphitic carbon are a major reason for catalyst deactivation. An analysis of the structure of adsorbed graphene thus has also some relevance for the understanding of the deactivation of catalyst surfaces. Graphene layers can also be formed by surface segregation of carbon by annealing carbon containing materials. The effect has been investigated, e.g., with carbon doped metals, but it often occurs also during the usual sputtering/annealing preparation of (nominally) clean metal crystals.[6–8] When applying this method one has to check if single or multilayers of graphite are formed because extended annealing leads to bulk graphite formation. In most cases the graphene layers are more or less randomly oriented with respect to an azimuthal rotation on the substrate surface, and ring structures in low-energy electron diffraction (LEED) patterns are regarded as a typical signature of surface graphite.[9] Clearly, this nonuniformity is unfavorable for the general application of such systems as templates.

Graphene on Ru(0001) may be different in this respect. In an early work on the Ru(0001) surface Grant and Haas observed during cleaning of the ruthenium sample, in particular after annealing to 1800 K, that the LEED pattern displayed hexagonal satellite spots.[10] The authors interpreted this phase as a (9×9) overlayer of graphite, formed by carbon segregation (but did not specify the thickness). Later Goodman and co-workers found in a scanning tunneling microscopy (STM) investigation of carbon species formed by decomposition of methane on Ru(0001) that, when the sample was subsequently annealed at 1300 K, a long-range surface structure appeared.[11] The lattice constant corresponded to an (11×11) superstructure, suggesting a moiré structure from the lattice mismatch between a single graphite layer and the Ru(0001) surface.

In this paper we present an investigation of graphene layers on Ru(0001) formed by surface segregation of carbon. The growth, structure and electronic properties of the films were investigated in detail using STM and scanning tunnel-

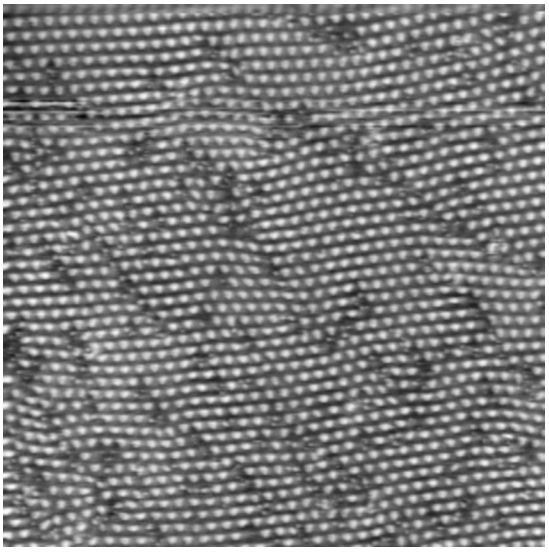

FIG. 1. STM image of Ru(0001) after annealing for 90 s to 1400 K, taken at room temperature. The quasihexagonal lattice is a graphene overlayer with a lattice constant of about 30 Å. 1000 Å × 1000 Å, I_t=3 nA, V_{sample}=−0.85 V.

ing spectroscopy (STS). Additional information was obtained from x-ray photoelectron spectroscopy (XPS), Auger electron spectroscopy (AES), and LEED.

II. EXPERIMENT

The experiments were performed in an ultrahigh vacuum (UHV) chamber at a base pressure of 1×10^{-10} mbar. A home-built beetle-type STM was used, which, by simultaneous He cooling and radiative counterheating from a hot filament at the backside of the crystal, can be operated at variable temperatures down to 55 K. The vacuum system is additionally equipped with a LEED optics and a cylindrical mirror analyzer for AES. Auger spectra were recorded with E_p=2000 V and a modulation voltage of 4 V peak-to-peak. XPS measurements were performed in a separate chamber, using a nonmonochromatized Mg $K\alpha$ source (1253.6 eV). (Source and analyzer at 36° with respect to the sample surface normal.)

The Ru(0001) sample (bought from MaTeck GmbH, purity 99.99%) was prepared by repeated cycles of argon ion sputtering at room temperature [p(Ar)=5×10^{-5} mbar, 1.0 keV], flash annealing to 1300 K, oxidation at 700 K [$p(O_2)=2\times10^{-7}$ mbar, 30 min], and reduction at 700 K [$p(H_2)=1\times10^{-6}$ mbar, 30 min]. After finally flash annealing to 1500 K the surface was clean and well ordered as checked with AES, LEED and STM. The graphene layers were prepared by prolonged annealing of the Ru(0001) sample to temperatures between 1000 and ⩾1400 K. Removal of the graphene layers was achieved by sputtering, whereas the standard oxidation process was too slow to completely remove the graphene.

III. PREPARATION OF THE GRAPHENE LAYERS

After annealing the cleaned sample for 90 s to 1400 K the 1000 Å × 1000 Å STM image of Fig. 1 was recorded.

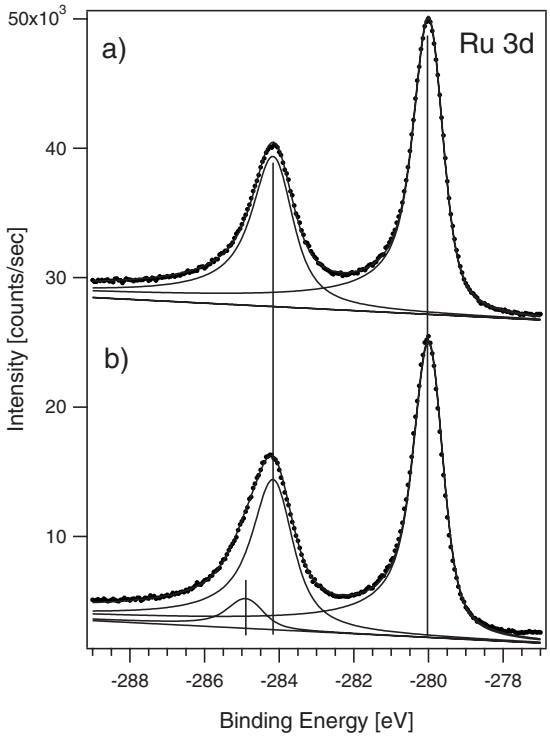

FIG. 2. (a) XPS of clean Ru(0001) and (b) of Ru(0001) after 90 s annealing to 1400 K, showing the binding energy region of the Ru $3d_{3/2}$ and Ru $3d_{5/2}$ states. The fit of spectrum (b) with the parameters of the clean Ru spectrum (a) (branching ratio, energies and widths of the Ru 3d doublet peaks, and background kept fixed) reveals two states under the left peak, the Ru $3d_{3/2}$ state at 284.1 eV and an additional component at 284.8 eV caused by the C 1s state of graphitic carbon.

The surface is covered with a superstructure forming a hexagonal lattice with a lattice constant of ~30 Å. The periodic structure also displays some angular distortions, mainly around dislocations in the overlayer, and there are also several translational domains. However, no areas of bare metal were observed after such prolonged annealing, so that the entire surface is covered by the same quasiperiodic superstructure. This structure was reproducibly formed by extended annealing, and the same type of STM images were obtained from the two other Ru(0001) samples investigated previously (one of which from a different producer, Surface Preparation Laboratory).

To identify the chemical species responsible for the overlayer structure XPS measurements were performed. Survey spectra exclusively showed Ru peaks. A difficulty is that the 1s state of carbon occurs at about the same energy as the Ru $3d_{3/2}$ peak, so that carbon cannot be identified by simple inspection of the spectra. Figure 2 shows the energy range of the Ru $3d_{3/2}/3d_{5/2}$ doublet. The doublet of the clean Ru surface [Fig. 2(a)] could be well fitted by two peaks, the Ru $3d_{3/2}$ state at 284.1 eV and the $3d_{5/2}$ state at 280.1 eV, and the expected branching ratio of 1.5 was obtained. By applying the same fit (same branching ratio, energies and widths of the Ru 3d doublet peaks, and background) for the annealed surface [Fig. 2(b)] it is found that the higher binding

energy peak contains an additional component centered around 284.8 eV. This is the typical energy of carbon in the graphitic form.[12] The overlayer must therefore consist of graphitic carbon that segregates from the bulk to the surface during the annealing. The moderate pressure rise during annealing (to $\sim 1 \times 10^{-9}$ mbar) rules out that the carbon originates from the residual gas.

As mentioned above, the XPS measurements had to be performed in a separate chamber. For these experiments the sample was transferred, after the annealing treatment, through air to the XPS chamber. The LEED pattern after the transfer showed the same overlayer spots as before (see below), evidencing that the overlayer is stable in air. Considering the chemical inertness of graphite and the difficulty of removing graphitic deposits from deactivated catalysts this property is not surprising.

AES was used to monitor the evolution of surface carbon as a function of annealing temperature (hold times between 90 and 120 s). Also for AES a complication arises from overlapping C and Ru transitions. However, the main feature of graphitic carbon in the differentiated spectrum, the *KLL* transition at 272 eV, is characterized by a relatively broad and pronounced negative going peak. The main peak of ruthenium, the *MNN* transition at 273 eV, is nearly symmetric [Fig. 3(a)]. Hence, the amount of carbon on Ru surfaces can be determined by measuring the ratio between the intensities of the lower and the upper half of the 273 eV peak [Fig. 3(b)].[13,14] In Fig. 3(c) this symmetry ratio is plotted vs annealing temperature. The freshly prepared clean surface displays a ratio of 1.3, which is in agreement with the standard data for Ru.[15] Prolonged annealing up to a temperature of 800 K is of no effect. Then, for temperatures between 1000 and 1400 K the ratio increases up to a value of 2.0, indicating the segregation of carbon to the surface.

STM images recorded after annealing to intermediate temperatures show islands. The image of Fig. 4(a) was taken after annealing to 1000 K for 120 s, corresponding to an AES peak symmetry ratio of 1.6, approximately in the middle between the clean and the fully covered surface. The islands display the same periodic overlayer as the structure in Fig. 1. The corrugation amplitude of the overlayer amounts to 0.7 Å (at negative tunneling voltages values of typically ~1.0 Å were found), the apparent average height of the islands above the metal terraces is 1.8 Å. For the geometric height of a graphene layer on Ru(0001) one would roughly expect a value of the order of 2.75 Å, corresponding to 1/2 times the graphite interlayer distance plus 1/2 times the Ru interlayer distance. One cannot expect to measure this value by STM because the electronic structures of graphene and the metal are very different. Compared to a metal, bulk graphite has a low density of states at E_F, and one may also expect a low density for adsorbed graphene. The effective barrier on bulk graphite is large because only high $\vec{k}_{\parallel}$ states contribute to the tunneling current.[16] A similar effect can be expected for adsorbed graphene, and it probably overcompensates the somewhat lower work function of Ru(0001)/graphene (4.5 eV) than of bare Ru(0001) (5.4 eV).[2] Irrespective of these electronic effects, which are both consistent with the low measured height, the data indicate that the islands are formed by single layers of graphite.

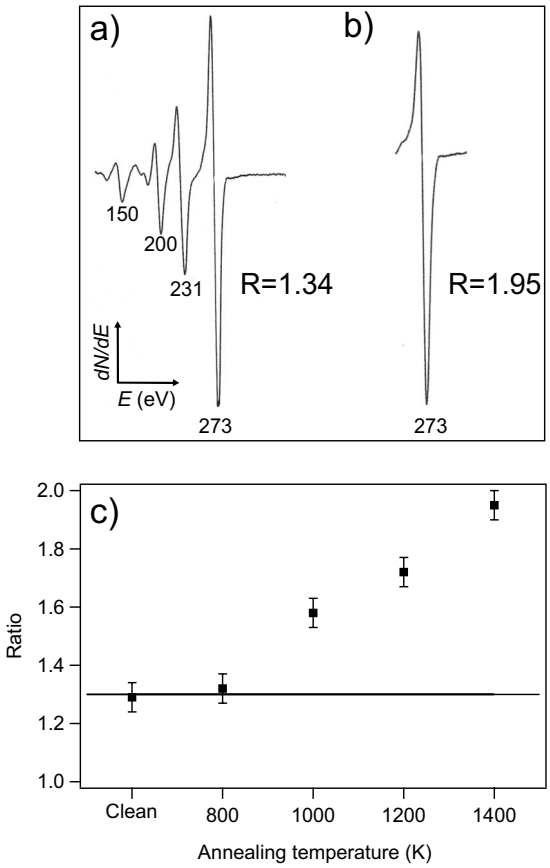

FIG. 3. Determination of the carbon coverage by AES. (a) dN/dE AES of clean Ru (Ru *MNN* transition at 273 eV) and (b) of the graphene covered surface after annealing. The enhanced asymmetry of the 273 eV peak is caused by the coinciding, strongly asymmetric C *KLL* transition). (c) Carbon coverage, determined from the ratio of the negative and positive going parts of the 273 eV peak in the dN/dE spectra. The increase between 800 and 1400 K shows the segregation of carbon.

The islands are exclusively found at the lower step edges of the ruthenium and are several hundred angstroms in diameter. This morphology is different from graphene islands grown by ethylene decomposition on Pt(111),[5] where, after annealing to 900 K, smaller, homogeneously distributed islands were observed that redistributed to larger islands along the step edges only by annealing to temperatures up to 1230 K. The difference appears to be caused by the different preparation procedures in the two cases.

After annealing to $T \geqslant 1400$ K the surface is fully covered with the overlayer [Fig. 4(b)]. As the height profile of this image shows [Fig. 4(c)] the steps are all 2.1 Å high, exactly the interlayer spacing of the (0001)-oriented Ru (2.14 Å), so that all steps must be steps of the Ru substrate. We have never observed graphite steps (3.35 Å) or another type of surface phase that could indicate graphite multilayers. (The corrugation in this measurement was 1.1 Å.) We conclude that under the chosen preparation conditions the segregation can be limited to a single graphene layer covering the entire surface. Effects that prohibit bulk growth could be of kinetic nature—the further segregation of carbon atoms below an

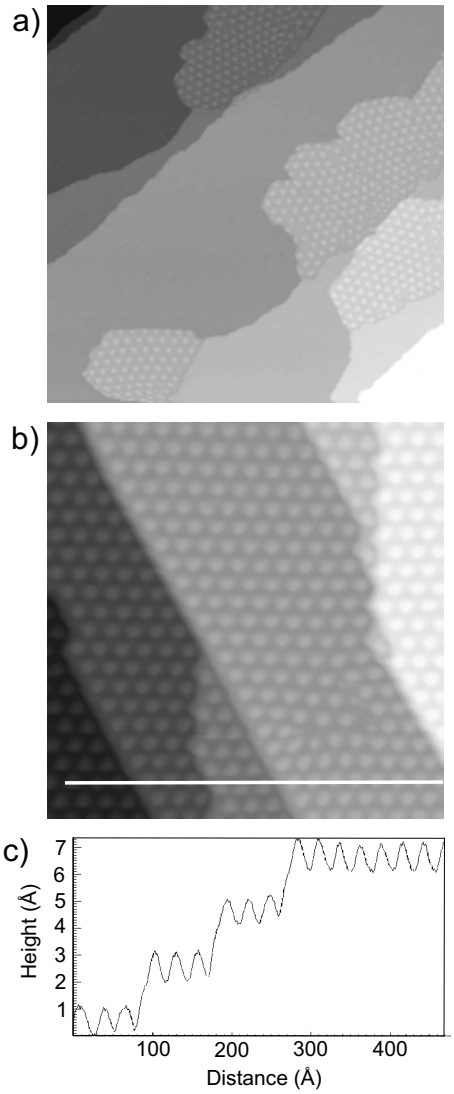

FIG. 4. STM images recorded after annealing at increasing temperatures. (a) After 120 s at 1000 K graphene has formed islands at the steps. 1000 Å × 1000 Å, I_t=1 nA, V_{sample}=−0.5 V. (b) After 90 s at 1470 K the surface is fully covered by graphene. 500 Å × 500 Å, I_t=1 nA, V_{sample}=−0.2 V. (c) Height profile along the line displayed in (b). The steps are ~2.1 Å high and thus represent steps of the Ru(0001) substrate. (b) shows that the Ru step edges are aligned along the main directions of the overlayer, indicating a restructuring of the underlying Ru surface.

existing coherent graphene layer is certainly energetically costly—or that the thermodynamic stability of bulk graphite is lower than of dissolved carbon atoms in Ru.

An interesting detail of Fig. 4(b) is the alignment of the steps along the main directions of the overlayer. Steps on bare Ru(0001) are typically bent with large radii,[17] as also seen in Fig. 4(a), but rarely show longer straight segments. Hence, the Ru surface restructures during the carbon segregation process to better adjust to the periodicity and orientation of the overlayer, indicating significant interactions between the graphene and the Ru surface.

IV. ATOMIC STRUCTURE OF THE GRAPHENE LAYER

Figure 5(a) shows an STM image with resolved atomic structure on the long-range overlayer and Fig. 5(b) a section with the overlaid honeycomb lattice of graphene on top (the two atoms A and B in the graphene unit cells shown as dots and crosses). One finds that 12 unit cells of the graphene correspond to one period of the long-range overlayer. This is also calculated from the measured ~30 Å periodicity which agrees with 12 times the lattice spacing of bulk graphite: 12 × 2.46 Å=29.5 Å. Almost the same value corresponds to 11 times the lattice spacing of Ru(0001): 11 × 2.71 Å =29.8 Å. It can be concluded that the long-range periodic structure represents a moiré structure formed by superposition of 12 graphene unit cells and 11 unit cells of the Ru(0001) surface. Because of the large size of the moiré unit cell (compared to typical atomically resolved STM images) and the slight distortions of the structure on longer length scales we cannot discriminate between a true (11 × 11) superstructure and an incommensurate structure of approximately the same periodicity. That graphene on Ru(0001) forms an (11 × 11) superstructure had been concluded before (from STM data without atomic resolution),[11] and similar moiré phases of graphene have been observed for Pt(111) and Ir(111).[1,5] The formation of moiré structures is a quite general phenomenon for adsorbed layers in which chemical bonds are strong within the layer and weaker to the underlying surface, as in metal/oxide and various other systems.[18–22]

Figure 5(a) shows that the graphene lattice and the moiré lattice are not rotated with respect to each other, so that the $[10\bar{1}0]$ directions of graphene and of Ru(0001) must be parallel. The distortions around dislocations in the moiré phase (Fig. 1) are connected with small rotations. Figure 5(c) shows such a case with atomic resolution. The atomic rows of the graphene are rotated by ~10° with respect to the moiré structure. However, the rotation between the two atomic lattices is much smaller, and the structure of Fig. 5(c) can be obtained by rotating the $[10\bar{1}0]$ direction of graphite by only 1° with respect to the $[10\bar{1}0]$ direction of ruthenium.[23] The periodicity of the moiré of ~30 Å is not measurably affected by this small rotation.

LEED [Fig. 6] confirms that the STM results are valid over macroscopic areas on the crystal. The diffraction pattern does not show the typical graphite rings or manifolds of rotational domains, but distinct satellites around the bright first order substrate spots. The overlayer periodicity of 11.6±0.2 substrate lattice constants from LEED is in reasonable agreement with the STM result. The previous observation of a (9 × 9) superstructure cannot be confirmed.[10] The width of the LEED spots in Fig. 6 may be explained by the finite distortions of the overlayer about the perfect periodicity.

Despite these distortions, the uniformity and alignment of the structure is surprising. In contrast, graphene overlayers on Pt(111) behave much more according to expectation from the binding properties of graphene, showing rotational angles between 0° and 90° and superstructure periodicities varying between 5 and 22 Å.[5] [The Ni(111)/graphene system is a special case because the very similar lattice constants of

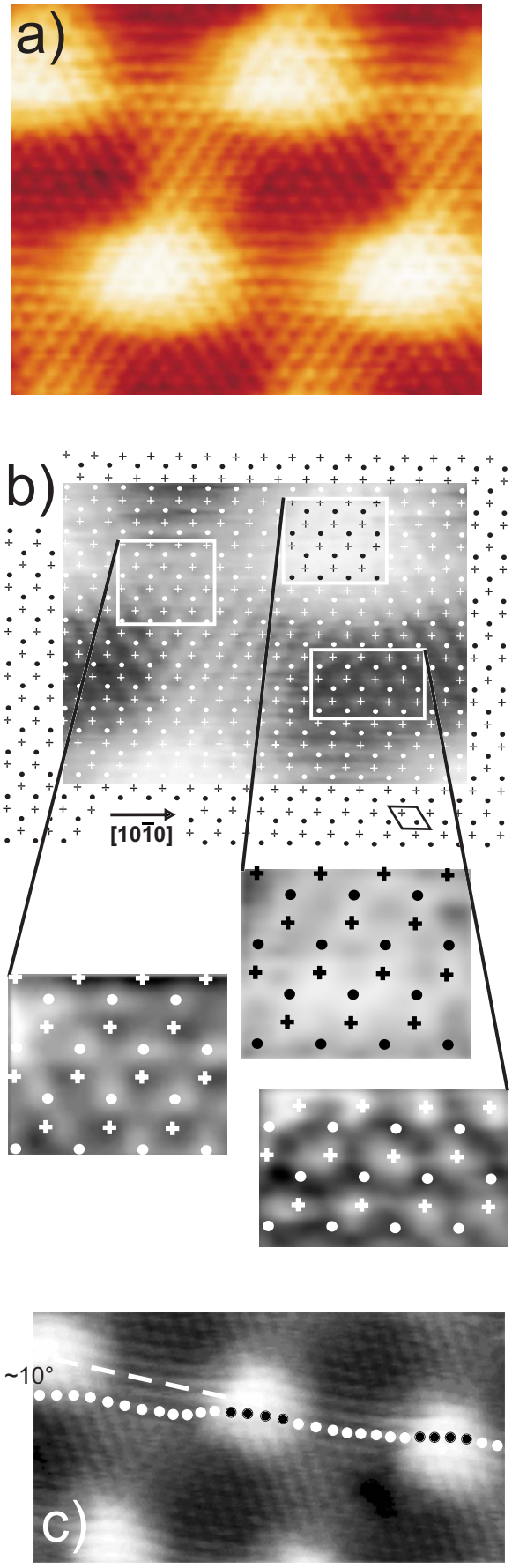

FIG. 5. (Color online) Atomically resolved images of the graphene overlayer. (a) The image shows three different levels of apparent heights, namely four bright maxima, a dark minimum in the center between the three maxima on the right hand side, and a less dark minimum between the three maxima on the left hand side. 50 Å $\times$40 Å, I_t=1 nA, V_{sample}=−0.05 V. (b) Section of (a) superimposed by the honeycomb lattice of graphene. Details from the three marked areas are enlarged. The two carbon atoms in the graphene unit cell, A and B, are displayed as dots and crosses, respectively. At the moiré maximum both atoms appear bright, so that the complete graphene hexagons are visible. In the darker half-cell the B atoms appear bright, in the less dark half-cell the A atoms. (c) STM image of a slightly rotated graphene layer. Using $\beta \cong \frac{a_{\text{Ru}}-a_{\text{C}}}{a_{\text{Ru}}}\alpha$ the measured angle $\alpha = \sim 10°$ between the moiré pattern and the graphene lattice can be transformed into the rotational angle $\beta = 1°$ between the ruthenium and the graphene lattice (a_{Ru} and a_{C} are the lattice constants of the Ru(0001) surface and of graphene). (Ref. 23) 40 Å $\times$80 Å, I_t=3 nA, V_{sample}=−0.05 V.

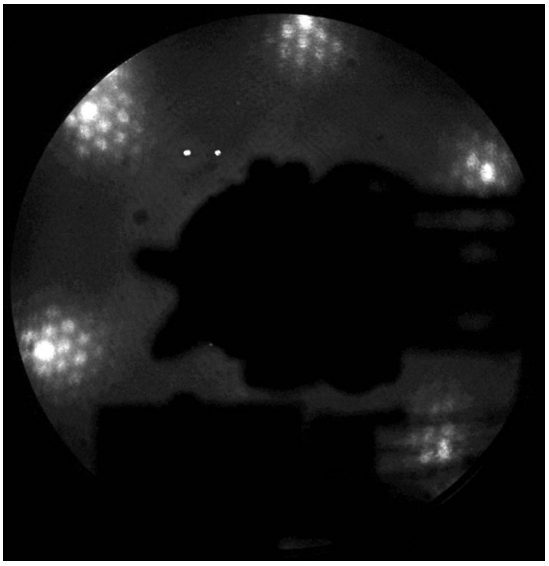

FIG. 6. LEED pattern of Ru(0001) after annealing to 1770 K. The bright substrate spots are surrounded by satellites caused by the graphene overlayer. Beam voltage 86 eV.

graphene and the metal lead to a (1×1) superstructure.[7,24]]

The model shown in Fig. 7 subsumes the main features of the moiré structure of graphene on Ru(0001) (assuming for simplicity a commensurate (11×11) superstructure and showing the main case of a perfect alignment of the $[10\bar{1}0]$ directions of graphite and ruthenium). Across the unit cell of the moiré structure the sites of the carbon atoms shift continuously with respect to the atoms of the Ru surface, giving rise to the long-range brightness modulation observed by

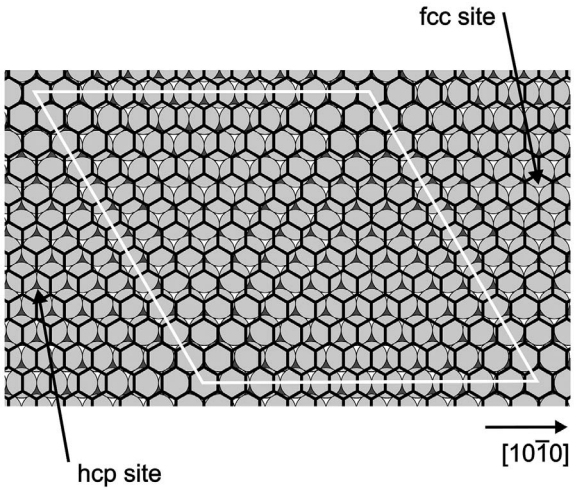

FIG. 7. Model of the overlayer structure of graphene on the Ru(0001) surface. The first layer Ru atoms are the light gray spheres, the second layer Ru atoms dark gray, and the graphene layer is the honeycomb net. The $[10\bar{1}0]$ direction of graphene is aligned with the $[10\bar{1}0]$ direction of ruthenium. The figure shows a commensurate (11×11) structure (with 12×12 graphene unit cells superimposed), but an incommensurate structure with very close periodicity is also possible.

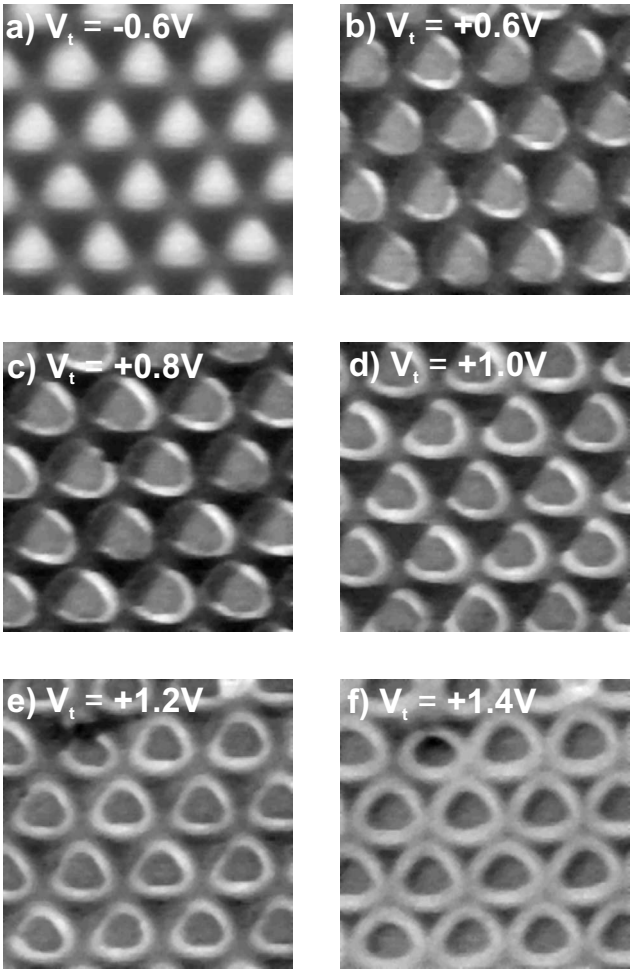

FIG. 8. STM images taken on the same area at varying bias voltages at 55 K. The sign refers to the sample, the tunneling current is the same in all images (I_t=1 nA). The appearance of the moiré changes from a hexagonal pattern of maxima for the filled states to bright rings for the empty states. The truncated appearance of the rings at intermediate voltages is probably an effect of an asymmetric tip and was not present in other measurements. 100 Å$\times$100 Å.

STM. Needless to say that one should be careful in interpreting the brightness modulation as a geometrical height variation of the carbon atoms.

Close inspection of Figs. 5(a) and 5(b) shows an important detail. According to the model (Fig. 7) there are three highly-symmetric arrangements of carbon atoms with respect to the underlying Ru atoms. At the corners of the moiré unit cell both carbon atoms, A and B, of the graphene are located above threefold hollow sites of the Ru surface. In the center of the right half-cell of the moiré unit cell the A atoms sit atop, and the B atoms above one type of threefold sites (say the fcc sites, as in Fig. 7). In the center of the left half-cell of the moiré the B atoms sit atop, and the A atoms above the other type of threefold sites (the hcp sites in Fig. 7). The STM [Fig. 5(a)] actually shows three such arrangements of atoms [see the highlighted windows in Fig. 5(b)]. The first appears at the bright maxima of the moiré structure, the second and third appear in the two roughly triangular minima in

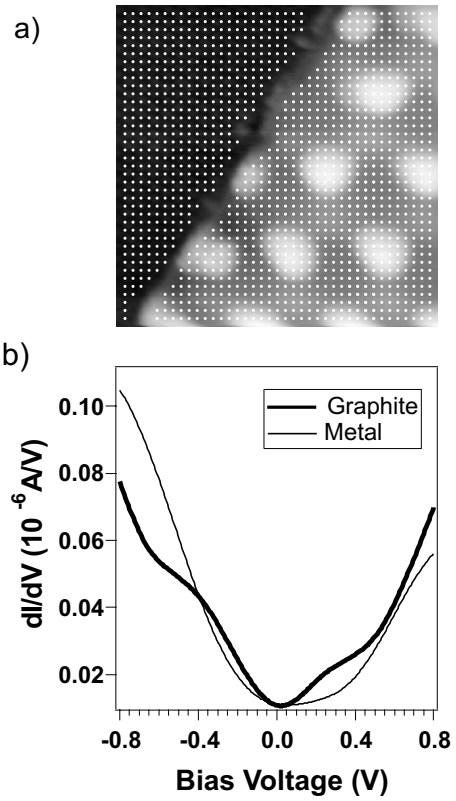

FIG. 9. STS measurements at the edge of a graphene island and on the surrounding metal surface. (a) Topographic image with superimposed grid where the spectra were taken. $I_t=1$ nA, $V_{\text{offset}}=-0.4$ V, 100 Å $\times$ 100 Å. (b) Averaged dI/dV spectra on the graphene area and on the metal. The graphene spectrum shows two peaks at −0.4 V and +0.2 V.

between, which clearly display two different average gray levels. On the moiré maximum [top right window in Fig. 5(b)], both atoms, A and B, appear bright, i.e., the full honeycomb rings of graphene are resolved. In the darker moiré minimum (lower right window) the B atoms appear bright, whereas the A atoms are not visible. In the less dark minimum (top left window) the A atoms appear bright, whereas the B atoms are not visible. Figure 7 is the only model consistent with these observations.

Such a contrast shift from one type of carbon atom to the other, with an intermediate imaging of both atoms, has not been reported before. In bulk graphite only one of the two types of atoms is resolved, i.e., the images do not show a honeycomb structure, but a hexagonal pattern. The common explanation is that in graphite the A and B atoms are not equivalent because the A atoms sit above the atoms of the second graphite layer, whereas the B atoms are located above the ring centers of the second layer.[25] The weak interlayer bond between the A atoms causes a band dispersion perpendicular to the surface and thus a lower state density at E_F at the A atoms, so that the B atoms dominate the imaging. However, the same asymmetry was reported for graphene on Pt(111) where this explanation is not applicable.[5] Other explanations have therefore been put forward,[26–28] but no generally accepted solution for this asymmetry problem of graphite has so far been reached. Our observations support an interpretation of the asymmetry in terms of interactions with the underlying layer. Evidently the shift in contrast from one type of atom to the other depends on the position with respect to the Ru substrate. One may speculate that the bright atoms in the three different high-symmetry positions in the moiré are those above the threefold sites because here, in an equivalent way as for bulk graphite, the bonding to the substrate is less strong, which may be related to a higher density of states at these atoms.

The corrugation of ~0.2 Å of the atomic lattice is in good agreement with the 0.21 Å hard-wall corrugation amplitude measured by He atom scattering (for bulk graphite).[29] The corrugation of 0.8 Å of the moiré in Fig. 5(a) is similar to the values from images without atomic resolution (at negative tunneling voltages). The moiré corrugation is significantly larger than the geometric buckling of 0.27 Å that was calculated for the graphene layer on Ir(111),[1] suggesting that electronic effects must play a role here.

V. ELECTRONIC EFFECTS

STM data taken at varying tunneling voltages show that electronic effects are indeed important. Figure 8 shows a series of images of the same area at bias voltages between −0.6 and +1.4 V (the sign refers to the sample). For −0.6 V [Fig. 8(a)] the typical moiré image is seen, a long-range hexagonal pattern of bright protrusions, and the two different minima, one appearing black, the other one less dark. Similar images were obtained between −2.0 and −0.2 V and are typical for the filled states. At small positive voltages [+0.6 V, Fig. 8(b)], so that empty states are imaged, the maxima become flat and develop bright rims. At more positive voltages [Figs. 8(c)–8(f)] the previous maxima become darker, finally turning into minima, and pronounced bright rings develop. (The truncated appearance of the rings at intermediate voltages is probably an effect of an asymmetric tip and was not present in other measurements.) Apparently, the imaging of the moiré structure displays strong electronic effects. (These measurements were performed at 55 K where the effect was easily visible. At room temperature it was difficult to obtain good data at positive voltages, but no systematic investigation of the temperature dependence was made.) Such an effect has not been seen before for other graphene systems.[30] Strikingly similar images were, however, observed for a boron nitride film on Rh(111),[18] for which originally a completely different structure model was proposed, but according to a recent theoretical study it may also be a moiré structure of a single layer.[22]

To gain more information about the electronic structure of the adsorbed graphene layer scanning tunneling spectroscopy (STS) data were taken. Because such measurements are often disturbed by tip artifacts we chose surface areas near graphene island edges, allowing us to check if electronic states vary between the graphene and the metal. Figure 9(a) shows the image of an island and the surrounding metal and the superimposed grid where the STS data were taken. The spectra were averaged over the graphene part and separately over the metal area, but defects and the immediate graphene/

metal edge region were excluded. As Fig. 9(b) shows, the spectrum on the metal area is structureless, as expected for a metallic surface where the density of states at a distance from the surface is dominated by *s* states. In contrast, the graphene area shows two states in the spectrum, one at approximately −0.4 V and a second at +0.2 V. That these states are absent on the metal confirms that they are caused by the graphene and not by some electronic state of the tip.

From the literature the electronic structure of adsorbed graphene layers near E_F is not very clear, and a definite interpretation of these measurements can presently not been offered. For an isolated graphene layer the π and π^* bands cross right at the *K* point of the Brillouin zone, giving rise to a single state at the Fermi energy.[31] This property is largely preserved for bulk graphite where it determines to a large extent the imaging by STM.[16] For adsorbed graphene basically two changes were observed by ultraviolet photoelectron spectroscopy and obtained in calculations, a downshift of the π system by 1 to 2 eV with respect to E_F, and a reorganization of the electronic structure at the *K* point.[2,4,32–35] For the (1×1) graphene overlayer on Ni(111) Souzu and Tsukada calculated the opening of a 1.0 eV wide gap at *K* centered at 0.8 eV below Fermi, which is caused by the coupling of the graphite π/π^* bands to the metal states near the *K* point.[36] Hence, a possible explanation for the two states in STS is that they represent the edges of such a gap resulting from the bond formation to the metal. The energies of the filled and the empty state are indeed asymmetric about 0 V, i.e., about E_F, although this asymmetry appears quite small considering the known energy downshifts of the π/π^* bands.

What might also play a role for the imaging of graphene is a 2D free electronlike state that for isolated graphene has density-of-states maxima above and below the layer.[37] For bulk graphite this state turns into a surface state that was identified by inverse photoelectron spectroscopy at +3.6 eV (at Γ).[38] STS data of bulk graphite displayed peaks in the same energy range, although the interpretation was somewhat controversial.[39,40] Because of the spatial distribution of the electron density this state should play a role for the interaction of graphene with a surface, and one may therefore expect an energy shift and a contribution to the tunneling current even at lower energies. The strange electronic effects observed by tunneling into empty states could thus possibly be connected with this surface state. What can be ruled out, however, is a contribution by image potential states that were shown to play an important role for ionic overlayers forming moiré phases.[19,20] Image potential states become crucial at tunneling voltages close to the barrier height, whereas in our case the electronic effects were visible already below 1 V.

VI. DISCUSSION

The surprisingly perfect orientation of the (11×11) graphene structure on the Ru(0001) surface, the absence of other moiré phases, and the restructuring of the metal underneath the full monolayer suggest a substantial interaction between graphene and ruthenium. This property is very likely essential for the homogeneity of the system, a precondition for its possible application as nanotemplate. The interaction must be considerably stronger than the interlayer bond in bulk graphite, following from the fact that multilayer segregation does not occur during completion of the monolayer. The strong electronic effects in the STM images of the moiré structure and the varying imaging of the A and B atoms depending on their positions above the metal atoms are both consistent with such a chemical interaction.

Quantitative data about the interaction strength between graphene and metal surfaces are only available from the most recent work on Ir(111).[1] An adsorption energy of 0.20 eV per carbon atom was obtained by calculations, a considerably higher value than the 50–60 meV interlayer binding energy in bulk graphite.[41] In an early theoretical work on Ru(0001)/graphene no stable adsorption of the layer was found, but this may be due to the artificial (1×1) structure that had been used.[42] Several systems showed a softening of in-plane phonons of adsorbed graphene compared to graphite, meaning that the C-C bonds are weakened, which, in turn, indicates stronger bonds to the substrate than in graphite.[11,43,44] The same conclusion can be drawn from the mentioned downshifts of the π/π^* bands with respect to graphite.

These data suggest a generally stronger interaction between graphene and various surfaces than the van der Waals interlayer interaction in graphite, but do not explain why Ru(0001) should be special. Here one can argue that, if the graphene-metal interaction actually has a covalent contribution, the same arguments about trends in bond strength as for chemisorbed atoms and molecules can be used.[45] Because of its higher-lying *d*-band Ru should form stronger bonds than Ir and Pt, which agrees with the rotational disorder in the case of Pt and the quite large metal-graphene distances reported for Pt(111) (3.70±0.05 Å)[9] and Ir(111) (3.77–4.04 Å).[1] Ni as a 3*d* metal should also form relatively strong bonds, and indeed very short layer distances were found [2.80±0.08 Å (Ref. 3) and 2.11–2.16 Å (Ref. 46)] [which, however, may be partially caused by the favorable (1×1) geometry].

VII. CONCLUSIONS

A graphene overlayer on Ru(0001) can be prepared without decomposing hydrocarbons, simply by prolonged annealing of the cleaned crystal in UHV to 1400 K, which leads to surface segregation of carbon atoms. The overlayer forms an (11×11) or very similar incommensurate structure. In contrast to the common rotational disorder of adsorbed graphene layers the overlayer shows a high degree of structural perfection, with good rotational alignment along the close-packed directions of the Ru surface and a well-defined periodicity of ~30 Å. The Ru crystal can be covered by a complete monolayer, without formation of other phases or of graphite multilayers. The properties of the system can be understood by stronger bonds to the Ru surface than the van der Waals interlayer bonds in graphite. The electronic structure is considerably altered with respect to isolated graphene and bulk graphite, and it also displays marked differences to other systems of adsorbed graphene. In contrast to previous STM investigations on bulk graphite and graphene layers both

carbon atoms in the graphene unit cell were resolved. The contrast between the two atoms varies, depending on their positions above the underlying Ru atoms. Despite the interactions with the underlying metal surface, the graphene layer on Ru(0001) maintains the chemical inertness of bulk graphite and was found to be stable in air. These properties make Ru(0001)/graphene a good candidate as template for engineering nanostructures.

*Author to whom correspondence should be addressed.

[1] A. T. N'Diaye, S. Bleikamp, P. J. Feibelman, and T. Michely, Phys. Rev. Lett. **97**, 215501 (2006).
[2] F. J. Himpsel, K. Christmann, P. Heimann, D. E. Eastman, and P. J. Feibelman, Surf. Sci. **115**, L159 (1982).
[3] R. Rosei, M. De Crescenzi, F. Sette, C. Quaresima, A. Savoia, and P. Perfetti, Phys. Rev. B **28**, 1161 (1983).
[4] C. F. McConville, D. P. Woodruff, and S. D. Kevan, Surf. Sci. **171**, L447 (1986).
[5] T. A. Land, T. Michely, R. J. Behm, J. C. Hemminger, and G. Comsa, Surf. Sci. **264**, 261 (1992).
[6] H. B. Lyon and G. A. Somorjai, J. Chem. Phys. **46**, 2539 (1967).
[7] J. C. Shelton, H. R. Patil, and J. M. Blakely, Surf. Sci. **43**, 493 (1974).
[8] J. C. Hamilton and J. M. Blakely, Surf. Sci. **91**, 199 (1980).
[9] Z.-P. Hu, D. F. Ogletree, M. A. Van Hove, and G. A. Somorjai, Surf. Sci. **180**, 433 (1987).
[10] J. T. Grant and T. W. Haas, Surf. Sci. **21**, 76 (1970).
[11] M. C. Wu, Q. Xu, and D. W. Goodmann, J. Phys. Chem. **98**, 5104 (1994).
[12] C. D. Wagner, W. M. Riggs, L. E. Davis, and J. F. Moulder, *Handbook of X-ray Photoelectron Spectroscopy* (Perkin Elmer, Eden Prairie, MN, 1979).
[13] M. J. Van Staden and J. P. Roux, Appl. Surf. Sci. **44**, 259 (1990).
[14] D. W. Goodmann and J. M. White, Surf. Sci. Lett. **90**, 201 (1979).
[15] L. E. Davis, N. C. MacDonald, P. W. Palmberg, G. E. Riach, and R. E. Weber, *Handbook of Auger Electron Spectroscopy*, 2nd ed. (Perkin Elmer, Eden Prairie, MN, 1978).
[16] J. Tersoff, Phys. Rev. Lett. **57**, 440 (1986).
[17] J. Wintterlin and T. Zambelli, Z. Phys. Chem. **219**, 997 (2005).
[18] M. Corso, W. Auwärter, M. Muntwiler, A. Tamai, T. Greber, and J. Osterwalder, Science **303**, 217 (2004).
[19] E. D. L. Rienks, N. Nilius, H.-P. Rust, and H.-J. Freund, Phys. Rev. B **71**, 241404(R) (2005).
[20] M. Pivetta, F. Patthey, M. Stengel, A. Baldereschi, and W.-D. Schneider, Phys. Rev. B **72**, 115404 (2005).
[21] A. Ueno, T. Fujita, M. Matsue, H. Yanagisawa, C. Oshima, F. Patthey, H.-C. Ploigt, W.-D. Schneider, and S. Otani, Surf. Sci. **600**, 3518 (2006).
[22] R. Laskowski, P. Blaha, T. Gallauner, and K. Schwarz, Phys. Rev. Lett. **98**, 106802 (2007).
[23] K. M. Ostyn and C. B. Carter, Surf. Sci. **121**, 360 (1982).
[24] C. Klink, I. Stensgaard, F. Besenbacher, and E. Lægsgaard, Surf. Sci. **342**, 250 (1995).
[25] D. Tománek, S. G. Louie, H. J. Mamin, D. W. Abraham, R. E. Thomson, E. Ganz, and J. Clarke, Phys. Rev. B **35**, 7790 (1987).
[26] A. L. Tchougreeff and R. Hoffmann, J. Phys. Chem. **96**, 8993 (1992).
[27] M.-H. Whangbo, W. Liang, J. Ren, S. N. Magonov, and A. Wawkuschewski, J. Phys. Chem. **98**, 7602 (1994).
[28] F. Atamny, O. Spillecke, and R. Schlögl, Phys. Chem. Chem. Phys. **1**, 4113 (1999).
[29] G. Boato, P. Cantini, and R. Tatarek, Phys. Rev. Lett. **40**, 887 (1978).
[30] There was one report of a contrast inversion of a moiré structure formed by graphene on TiC(111), H. Itoh, T. Ichinose, C. Oshima, T. Ichinokawa, and T. Aizawa, Surf. Sci. **254**, L437 (1991), and a moiré structure of bulk graphite also showed a strong tunneling voltage effect, Z. Y. Rong and P. Kuiper, Phys. Rev. B **48**, 17427 (1993).
[31] P. R. Wallace, Phys. Rev. **71**, 622 (1947).
[32] R. Rosei, S. Modesti, F. Sette, C. Quaresima, A. Savoia, and P. Perfetti, Phys. Rev. B **29**, 3416 (1984).
[33] K. Kobayashi and M. Tsukada, Phys. Rev. B **49**, 7660 (1994).
[34] A. Nagashima, H. Itoh, T. Ichinokawa, C. Oshima, and S. Otani, Phys. Rev. B **50**, 4756 (1994).
[35] A. Nagashima, N. Tejima, Y. Gamou, T. Kawai, and C. Oshima, Phys. Rev. B **51**, 4606 (1995).
[36] Y. Souzu and M. Tsukada, Surf. Sci. **326**, 42 (1995).
[37] M. Posternak, A. Baldereschi, A. J. Freeman, and E. Wimmer, Phys. Rev. Lett. **52**, 863 (1984).
[38] T. Fauster, F. J. Himpsel, J. E. Fischer, and E. W. Plummer, Phys. Rev. Lett. **51**, 430 (1983).
[39] B. Reihl, J. K. Gimzewski, J. M. Nicholls, and E. Tosatti, Phys. Rev. B **33**, 5770 (1986).
[40] Z. Klusek, Appl. Surf. Sci. **151**, 251 (1999).
[41] M. Hasegawa and K. Nishidate, Phys. Rev. B **70**, 205431 (2004).
[42] P. Feibelman, Surf. Sci. **103**, L149 (1981).
[43] T. Aizawa, R. Souda, Y. Ishizawa, H. Hirano, T. Yamada, K.-I. Tanaka, and C. Oshima, Surf. Sci. **237**, 194 (1990).
[44] T. Aizawa, R. Souda, S. Otani, Y. Ishizawa, and C. Oshima, Phys. Rev. Lett. **64**, 768 (1990).
[45] B. Hammer and J. K. Nørskov, Adv. Catal. **45**, 71 (2000).
[46] Y. Gamo, A. Nagashima, M. Wakabayashi, M. Terai, and C. Oshima, Surf. Sci. **374**, 61 (1997).